Biomass and Bioenergy 198 (2025) 107871

Contents lists available at ScienceDirect

Biomass and Bioenergy

journal homepage: www.elsevier.com/locate/biombioe

Techno-economic assessment of a plant for the upgrading of MSW biogas to synthetic natural gas by thermocatalytic methanation

P. Sanz-Monreal, V.D. Mercader, P. Aragüés-Aldea, P. Durán, E. Francés, J. Herguido, J.A. Peña *

Catalysis and Reactor Engineering Group (CREG), Aragon Institute of Engineering Research (I3A), Universidad Zaragoza, C/ Mariano Esquillor s/n, 50018, Zaragoza, Spain

ARTICLE INFO

Keywords:
CO_2 methanation
Biogas upgrading
Technoeconomic assessment
Renewable hydrogen
Synthetic natural gas

ABSTRACT

This study evaluates the techno-economic feasibility of a plant designed to produce synthetic natural gas (SNG) from biogas through direct catalytic methanation. The proposed facility is simulated with *Aspen Plus*® v14, using a comprehensive approach that covers the entire process, from biogas pretreatment to the production of the final product. The installation aims to contribute to the development of *Power-to-Gas* (*Power-to-Methane*) strategy for decarbonization.

The plant, to be located in northeastern Spain, operates at an industrial scale with a production capacity of approximately 1100 Nm^3/h of SNG, obtained from a 1425 Nm^3/h biogas plant. The process includes five main stages to meet Spanish gas quality standards for grid injection: desulfurization, using amines for sulfur removal; electrolysis, for the generation of renewable hydrogen; thermocatalytic methanation, which combines CO_2 from the biogas with hydrogen to enrich the methane content; dehydration, to meet SNG moisture specifications; and cogeneration, intended for the joint production of electricity and steam to meet the plant's energy demands.

A detailed analysis of investment costs (CAPEX) and operational expenses (OPEX) is conducted, identifying the key factors influencing the project's profitability. The economic assessment indicates a total capital investment of 21.83 M€ and operational expenses nearly 8 M€ annually. The profitability threshold for the base scenario is estimated at 91.75 €/MWh, exceeding the 2023 natural gas market average in the Iberic peninsula (39.11 €/MWh), highlighting the current economic challenges of SNG production.

List of acronyms

Abbreviation	Full form
AEL	Alkaline Electrolysis
AEM	Anion Exchange Membrane Electrolysis
APEA	Aspen Process Economic Analyzer
CAPEX	Capital Expenditures
CEPCI	Chemical Engineering Plant Cost Index
COM	Cost of Manufacture
DW&B	Direct Wages and Benefits
EBITDA	Earnings Before Interest, Taxes, Depreciation, and Amortization
EU	European Union
GE	Total General Expenses
GHSV	Gas Hourly Space Velocity
HHV	Higher Heating Value
LHHW	Langmuir-Hinshelwood-Hougen-Watson

(*continued on next column*)

(*continued*)

Abbreviation	Full form
M&O-SW&B	Combined Salary, Wages, and Benefits for Maintenance and Labor-related Operations
MIBGAS	Iberian Gas Market
MW&B	Maintenance Wages and Benefits
NGTS	Technical Management Standards of the System
OPEX	Operational Expenses
PD	Detailed Protocol
PEM	Polymer Electrolyte Membrane
PtM	Power to Methane
ROI	Return on Investment
SEDIGAS	Spanish Gas Association
SNG	Synthetic Natural Gas
SNR	Renewable Natural Gas
SOEC	Solid Oxide Electrolysis

(*continued on next page*)

This article is part of a special issue entitled: Rafael Bilbao published in Biomass and Bioenergy.

* Corresponding author.
E-mail address: jap@unizar.es (J.A. Peña).

https://doi.org/10.1016/j.biombioe.2025.107871
Received 14 February 2025; Received in revised form 3 April 2025; Accepted 3 April 2025
Available online 10 April 2025

(*continued*)

Abbreviation	Full form
TSA	Temperature Swing Adsorption
TPI	Total Permanent Investment
WC	Working Capital

1. Introduction

The transition to a sustainable energy model and the reduction of greenhouse gas emissions, particularly carbon dioxide and methane, is a global priority in the fight against climate change [1]. Renewable energy sources have emerged as a key component of this transition, with their implementation significantly increasing over the past decade. These energy sources support the decarbonization of the energy sector and favor the creation of decentralized energy networks, which are often more resilient to fluctuations in external energy markets [2]. However, renewable energy technologies face significant limitations, primarily due to their reliance on intermittent sources. This intermittency presents challenges for maintaining a consistent energy supply, since atmospheric conditions are to some extent unpredictable, and overall, beyond human control. Under favorable weather conditions, renewable energy systems can generate more electricity than the grid can accommodate, leading to energy wastage that could otherwise be harnessed for various applications [3].

A promising solution to address these challenges involves converting surplus energy into alternative energy carriers, such as hydrogen. Hydrogen has been identified as a critical energy vector with the potential to overcome the limitations of renewable energy systems by enabling its use in strategic sectors and applications that are difficult to electrify (e.g steel, cement, chemicals and ceramic manufacturing, ammonia production, heavy transport, and in general, high-temperature processes) [4]. Moreover, hydrogen plays a pivotal role in reducing greenhouse gas emissions and replacing fossil fuels [5]. Despite its potential, the widespread adoption of hydrogen production and applications remains challenging. While technological advancements and declining energy costs are expected to reduce the price of renewable hydrogen production significantly [6], achieving cost competitiveness with conventional fossil fuels remains a difficult hurdle. Additionally, the complexity of handling, transporting, and storing the gas after its production further adds to these challenges [7].

In order to facilitate the green energy transition to hydrogen, carriers with higher energy density, such as synthetic methane (or *synthetic/renewable natural gas* -SNG/RNG-), methanol, or ammonia, may play a crucial role [8,9]. Among them, methane offers the easiest integration into the already existing energy supply system, as it is comparable to the current fossil natural gas and so, it can be introduced into the existing natural gas network. Additionally, SNG is safer and easier to store, reducing economic costs compared to hydrogen. In this scenario, *Power-to-Methane* (PtM) provides innovative solutions to utilize surplus renewable energy. This process converts excess electrical energy into green hydrogen through water electrolysis, which then reacts with CO_2 to produce methane (SNG) via the *Sabatier* reaction (r.1) [10]. Thus, PtM enables the capture, storage, and reuse of CO_2, contributing to the circular economy and decarbonizing strategic sectors where electrification is unpracticable (glass, ceramic or steel industries), or in processes where the generation of CO_2 is an inherent characteristic of the manufacturing processes itself, such as the cement industry.

$$CO_{2\,(g)} + 4H_{2\,(g)} \rightleftharpoons CH_{4\,(g)} + 2H_2O_{\,(g)}\,;\, \Delta H^0_{Sabat} = -165.1\left[kJ{\cdot}mol^{-1}\right] \qquad (r.1)$$

In thermocatalytic methanation, the most commonly active phase are metals such as Co, Pd, Rh, Ru, and Ni. These catalysts are typically supported on high-surface-area materials (Al_2O_3, ZrO_2, zeolites, etc.) to enhance their exposure to reactants. Among them, ruthenium stands out as the most active catalyst; however, its high cost and limited availability could obstacle its large-scale industrial application. In contrast, nickel-based catalysts have demonstrated high effectiveness despite their lower cost and greater availability, widely used option in commercial applications. Additionally, the incorporation of a second metal (bimetallic catalysts), such as Fe, has been shown to improve reaction performance [11].

Reactor design is another critical aspect. In general, the most relevant reactor configurations are fixed-bed, monolith, microchannel, membrane and sorption-enhanced [12]. Fixed-bed reactors are the most widely used due to their simple design, scalability, and cost-effectiveness. They are the preferred choice for gas-phase catalytic processes, except in cases where heat transfer limitations or catalyst deactivation pose significant challenges. One of the primary issues in methanation is the removal of the heat generated, as well as the formation of hot spots along the reactor bed that can lead to carbon deposition, carbon monoxide production, catalyst sintering, and subsequent deactivation [13]. To address this, different cooling strategies have been developed, ranging from reactant distribution and dilution to optimized heat exchange mechanisms involving coolant selection and flow configuration [14].

On the other hand, biogas emerges as a renewable source of CO_2 as well as a waste product. If left untreated, it worsens the problem of increasing atmospheric concentrations; not only of CO_2 but also of CH_4, which is significantly more harmful than CO_2 itself as a greenhouse effect contributor [15]. Biogas is the result of the anaerobic decomposition of organic matter, being forestry, cattle, agricultural, sewage sludge or urban wastes the most common. According to its origin, its composition slightly varies, being a mixture of CH_4 (55–70 %^{v}), CO_2 (30–45 %^{v}) and several minor impurities (H_2S, H_2O, NH_3, etc.) [16]. This composition makes it ideal for being "*upgraded*" in its CH_4 content, allowing its integration into the natural gas network [17–19]. However, while European regulations establish common requirements and testing methods for biomethane injection [20,21], the specific conditions for grid connection and biomethane injection differ across countries. Key factors -including gas quality standards, injection fees, and cost-sharing agreements between grid operators and biomethane producers-significantly influence the development and viability of biomethane plants [22]. For instance, the minimum methane content required in Germany (98 %) [23,24] or Denmark (97 %) [25] is significantly higher compared to countries like the Netherlands (85 %) or Spain (90 %) [26].

Spain, with its substantial renewable energy generation capacity, has positioned as a leader in solar and wind energy production in Europe, reflecting a steadfast commitment to the energy transition [27]. The Iberian Peninsula boasts the third-highest solar radiation intensity within the European Union (EU) [28], receiving an average of 4.58 kWh/m^2 per day. Within the continent, only Cyprus and Malta surpass these values; however, their limited land area and lack of interconnections constrain their ability to fully exploit their solar potential. Spain also benefits from favorable wind resources, as evidenced by wind energy contributing 23.5 % of the country's electricity demand in 2023 [29], with several locations exceeding 800 W/m^2 [30]. Despite these advancements in renewable energy, the development of biogas and biomethane has remained limited, even though Spain possesses a significant biomass supply. According to a report by the *Spanish Gas Association* (SEDIGAS), up to 2326 potential sites for biomethane production have been identified across the country [31]. However, only 2 % of Spain's estimated biomethane production capacity is currently being utilized, placing it behind countries such as Germany or France [32]. The suspension of incentives in 2012 (*Real Decreto-ley 1/2012,* [33]) and the lack of an effective support framework have hindered the commissioning of new biogas and biomethane plants, resulting in production targets that are well below the nation's full potential. Although the *Biogas Roadmap* ("*Hoja de Ruta del Biogás*" [34]) and the *Climate Change Law* signal future improvements, current support mechanisms remain practically nonexistent, leaving Spain behind other European countries

with more consolidated policies. Consequently, this underutilization of biomass resources highlights the need for targeted policies and incentives to foster the valorization of this critical energy vector.

Several recent techno-economic studies have addressed PtM systems [35–40]. However, these works generally explore discrete configurations, specific electricity pricing assumptions, or smaller production scales, leaving a gap in understanding how industrial-scale PtM plants -particularly those integrating municipal solid waste (MSW) biogas-perform in a Spanish context. Our research addresses this gap by analyzing an industrial-scale PtM facility co-located with an MSW biogas source, providing a comprehensive techno-economic assessment (e.g., CAPEX, OPEX, profitability thresholds) under Spain's regulatory and market framework. The analysis is framed within the broader context of the energy transition and aims to contribute valuable insights into the development of sustainable solutions for a renewable-based economy.

2. Methodology

The biogas upgrading plant for synthetic natural gas production via catalytic methanation was modeled using *Aspen Plus*® (v14) to design the process and perform mass and energy balance calculations. The configuration of the plant is comprised of five primary sections: biogas desulfurization, water electrolysis, catalytic methanation, SNG dehydration, and cogeneration (see Fig. 1). The *ELECNRTL* (*Electrolyte Non-Random Two Liquids*) property method was used for the desulfurization and electrolysis zones, while *CPA* (*Cubic-Plus-Association*) was used for the dehydration zone and *PR-BM* (*Peng-Robinson-Boston-Mathias*) for the remaining units. *Aspen Plus*® flow diagrams and stream tables are provided as Supplementary Material. Each location was analyzed from a technical perspective to ensure that the generated gas, prior to injection, complies with the regulatory requirements established by Spanish gas legislation. Subsequently, a preliminary economic assessment was conducted, considering both capital investment costs (CAPEX) and operational costs (OPEX) to evaluate the techno-economic feasibility of the system and determine the production cost of SNG that yields either 0 or 20 % ROI. The cost analysis has been set for the year 2023, based on data and information consolidated during this period.

The facility is planned to be located in the northeastern Spain area, within the *Ebro Valley* region. The biogas digesters process solid wastes generated by approximately 750,000 inhabitants, generating a feed of approximately 1425 Nm^3/h of raw biogas (12,500,000 Nm^3/year). A representative composition of the biogas produced is detailed in Table 1.

The synthetic natural gas production capacity is approximately 1100 Nm^3/h. Reported production plants typically operate within a range of 1–325 N m^3/h [41]. Therefore, the modeled facility significantly exceeds pilot-scale methanation plants, positioning on an industrial scale. The plant is assumed to have a 20-year operational lifespan, with 8000 operating hours per year, corresponding to 91.3 % production capacity, consistent with previous techno-economic analyses [42,43]. The requirements for injecting gas into the Spanish gas system are defined by the *Technical Management Standards of the Gas System* (NGTS). These regulations establish the general conditions for the use of gas infrastructure, providing key operational guidelines. The standards (see Table 2) are specially detailed in Protocol PD-01, which addresses *Measurement, Gas Quality, and Odorization* of the gas [44]. Gases from non-conventional sources, such as biogas, biomass-derived gas, or other gases produced through microbial digestion processes, are subject to additional quality specifications (see Table 2) [45]. Further information regarding the *Wobbe Index*, *Higher Heating Value* (*HHV*), and the *Relative*

Table 1
Composition of raw biogas.

Species	Concentration (%^{v})
CH_4	54.5
CO_2	42.0
N_2	2.7
O_2	0.7
H_2S	0.1

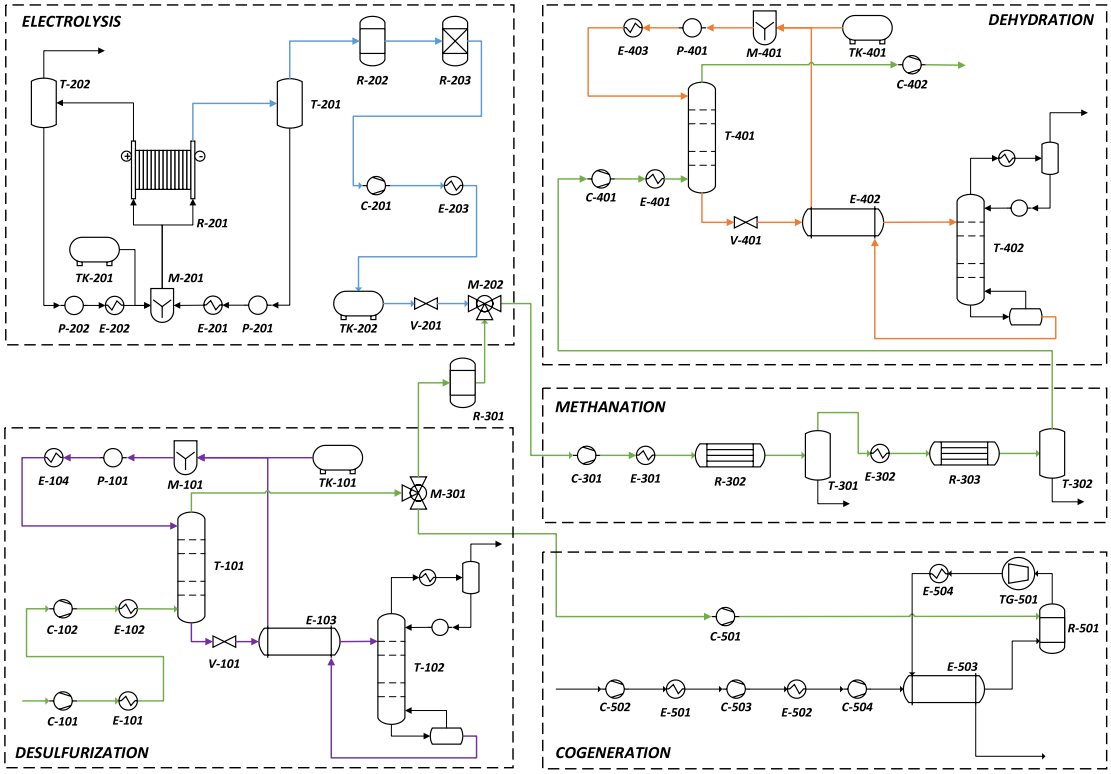

Fig. 1. Picture flowsheet diagram (PFD) of the installation. Blocks surrounded by dashes show representative sections of the process.

Table 2
Gas quality requirements for injection into the Spanish grid [44,45].

Property (*)	Units	Min.	Max.
Wobbe Index	kWh/m^3	13.403	16.058
Higher Heating Value (HHV)	kWh/m^3	10.26	13.26
Relative Density	–	0.555	0.700
Total Sulfur (excluding odorant)	mg/m^3	N/A	50
H_2S + COS (as sulfur)	mg/m^3	N/A	15
RSH (as sulfur)	mg/m^3	N/A	17
O_2	mol/mol	N/A	0.001 %
CO_2	mol/mol	N/A	2.5 %
CH_4	mol/mol	90 %	N/A
CO	mol/mol	N/A	2 %
H_2	mol/mol	N/A	5 %
Water Dew Point	°C at 70 bar (a)	N/A	+2
Hydrocarbon Dew Point	°C at 1–70 bar (a)	N/A	+5

(*) Properties are expressed under the following reference conditions: [0 °C; V (0 °C; 1.01325 bar)].

Density can be found in the Supplementary Material.

Additional installation costs include a cooling water service provided via a cooling tower. Although electricity and high-pressure steam are generated on-site, the electrolyzer operates with electricity sourced from the grid. It is assumed that 37.5 % of the electricity supply comes from renewable sources, based on Spain's 2023 energy mix (23.5 % wind [46], 14 % photovoltaic [47]). During this period, electricity costs are considered negligible in terms of operational expenses, accounting only for periods when neither renewable source contributes to the grid. The capital expenditure (CAPEX) for the renewable plant is excluded from the analysis; however, the electrolyzer itself is included in the investment costs. Steam production does not contribute into operational costs, as it is produced taking advantage of the heat coming from the reactors (exotherm reactions) and a boiler within the cogeneration zone. All auxiliary services are treated as "virtual," meaning they rely on shared utility systems without dedicated infrastructure.

The heat exchangers modeled for the facility are of two types: simple (*Heat* model) and rigorous (*HeatX* model). Simple exchangers are used for integration between process streams and auxiliary service streams, while rigorous models are utilized for interactions between process streams. For heat exchangers utilizing cooling water as the heat exchange medium, as well as those facilitating heat transfer between process streams, a minimum temperature difference (ΔT_{min}) of 5 °C has been considered. However, for exchangers utilizing high-pressure steam, ΔT_{min} has been increased to 10 °C. Pressure losses are estimated in 10.3 kPa for processes involving phase change and 41.4 kPa for all other cases [48].

The isentropic efficiency of compressors (*Compr* model as Compressor) is set at 85 %, while turbines (*Compr* model as Turbine) operate at an isentropic efficiency of 90 % [49]. Conversely, pumps (*Pump* model) are assumed to have a typical mechanical efficiency of 75 % [50]. The power generated by the turbine is distributed between the compression train used in the cogeneration unit and an electrical generator. The generator supplies power to pumps, compressors, and the cooling system. The efficiency of converting turbine-generated work into electricity is assumed to be 100 %. Except for the compression stages within the cogeneration unit, which are powered by the turbine, all other compression stages and pumps derive their mechanical power from electric motors. The mechanical efficiency (ratio of mechanical energy output to electrical energy input) of the motors is assumed to be 90 % for compressors and 75 % for pumps [51].

3. Description of the process and system boundaries

The following chapter describes the process of upgrading biogas to synthetic natural gas, distinguishing the different sections by their function within the system as well as their limits. It also includes a subchapter devoted to the economic analysis of the whole process, and a brief description of the methodology employed to that end.

3.1. Desulfurization

Biogas purification is a critical step in the production of synthetic natural gas via catalytic methanation, particularly for the removal of sulfur-containing compounds such as hydrogen sulfide (H_2S) and organic sulfur molecules. These compounds not only reduce methanation efficiency but also pose regulatory challenges for SNG injection into the natural gas grid. According to regulations [44], the sulfur content in SNG must be below 50 mg S/Nm^3 (considering odorization). Besides, to protect nickel- or ruthenium-based methanation catalysts, an even stricter concentration limit of less than 0.1 ppm should be required [52].

While various desulfurization technologies are available in the oil and gas industry, no single solution dominates for applications like catalytic methanation [53]. For moderate sulfur compound concentrations, adsorption methods such as sacrificial iron or zinc oxide beds are commonly used, where the oxide reacts with H_2S to form the metallic sulfide which is retained by the bed as solid. However, for high H_2S concentrations typical of raw biogas, or facilities in which a high volume of biogas must be processed, chemical absorption techniques are more efficient and reliable [54]. In this study, chemical absorption using amines was selected as the most suitable desulfurization technology. However, a challenge inherent to this method is the potential co-absorption of CO_2, an essential reactant for methanation. Therefore, careful selection of the amine solvent is crucial. In this case, *methyl diethanolamine* (MDEA) was chosen due to its high selectivity for H_2S and low affinity for CO_2 [55].

The desulfurization process is conducted in a system comprising an absorber (T-101) and a regeneration column (T-102), connected by a heat exchanger (E-103) for energy integration. In the absorber, raw biogas flows (from bottom) counter currently with the MDEA solution (from top), transferring H_2S into the solvent. The H_2S-rich amine is then regenerated in the desorption column, where H_2S is released, allowing the regenerated solution to be recirculated to the absorber [54]. The absorber (T-101) and rectification columns (T-102) (Table 3) are simulated using *RadFrac* models available in *Aspen Plus*®. The employed calculation method (*Equilibrium*) is the standard approach for this type of equipment. Pressure drop per tray is estimated at 0.7 kPa [48]. All columns incorporate 20 sieve trays with a standard spacing of 24 inches. The program determines the column diameter to prevent "drying up" issues and achieves approximately 80 % flood level. Key operating parameters were selected based on specialized literature, while solvent flow rate (4445 kg/h) and concentration (50 %^{w}) were optimized reducing equipment sizing and energy and heat requirements. The desulfurized biogas is primarily directed to the methanation section, while a small fraction (~10 %^{v}) is diverted to the cogeneration unit for on-site heat and electricity production.

3.2. Electrolysis

Renewable hydrogen production via electrolysis is a crucial stage in

Table 3
Properties of the desulfurization section columns.

Property	Unit	T-101	T-102
Number of trays	trays	20	20
Solution inlet temperature	°C	35	184.1
Operating temperature	°C	61.0–59.1	45.0–119.8
Operating pressure	kPa	800–786	101.3–167
Tray spacing	m	0.6096	0.6096
Internal diameter	m	0.306	0.347
Tray type	adim.	Sieve	Sieve
Tray height	m	12.19	12.19
Total height	m	13.21	13.42
% Flooding	adim.	80	80

the methanation process, as it determines both the efficiency and overall cost of the plant. Various electrolysis technologies are available, with the most commercially established being alkaline electrolysis (AEL) and polymer electrolyte membrane (PEM) electrolysis. Additionally, solid oxide electrolysis (SOEC) and anion exchange membrane (AEM) electrolysis are in pre-commercial stages [56].

Alkaline electrolysis uses a concentrated alkaline solution -commonly potassium hydroxide (KOH)- as the electrolyte, with electrodes immersed in the solution and separated by a diaphragm that allows hydroxide ions (OH^-) to migrate from the cathode to the anode. This technology is currently the most mature and cost-effective, offering high efficiency and the capability to produce hydrogen at scales of up to 5 MW per stack [57]. However, the use of corrosive alkaline solutions increases maintenance costs, and alkaline systems generally require stable load operation because of their slow startup times [58]. In contrast, PEM (*Proton Exchange Membrane*) electrolyzers incorporate a proton-conducting polymer membrane (e.g., *Nafion*®) as both separator and electrolyte, enabling faster startup (1–5 min) and flexible adaptation to the intermittency of renewable energy [57]. However, PEM systems often rely on precious metal catalysts, raising capital costs, though future price reductions are anticipated [59]. Given the need to produce hydrogen at large scale, alkaline electrolysis was selected for this project due to its high technological maturity, lower operating costs, and ability to produce large hydrogen volumes.

The electrolyzer system (R-201, Table 3) was modeled using the *Electrolyzer* model in *Aspen Plus*®, employing a potassium hydroxide solution as electrolyte. Additionally, a 20-bar buffer tank (TK-202) was incorporated downstream to smooth operational fluctuations and ensure a continuous hydrogen supply to the methanation reactors. This storage capacity allows the methanation plant to operate for 1 h without electrolytic hydrogen production [60]. Water containing the electrolyte (TK-201) is separated into hydrogen and oxygen, with the resulting streams subjected to further treatment. Hydrogen undergoes deoxidation catalytic reactor (*deoxo*) (R-202, as a *RGibbs* model) to remove oxygen traces, followed by temperature swing adsorption (TSA) purification (R-203, as a *Separator* model) to remove water. The purity of H_2 is assumed to be around 100 %, as alkaline electrolyzers can achieve this level with appropriate auxiliary equipment [61].

The electrolyzer design was optimized to produce hydrogen in a stoichiometric ratio with the CO_2 derived from biogas. The main operating conditions (Table 4) include a pressure of 10 bar, a temperature of 50 °C, and an energy efficiency of 80 % based on the higher heating value (HHV) [62,63]. Water consumption and power requirements are directly related to hydrogen production, reaching 1160 kg/h of water consumption and 6.4 MW of electrical power.

3.3. Methanation

Before entering the methanation reactors, the purified biogas (33 %^{v} CO_2; 61 %^{v} CH_4; 3 %^{v} N_2; 0.68 %^{v} O_2; 2.32 %^{v} H_2O – note H_2O arises from partial saturation of the gas during amine scrubbing) is mixed with hydrogen in a stoichiometric ratio respect CO_2 (4:1), with both compounds being diluted in the original CH_4 coming from the biogas. However, due to the small fraction of oxygen present in the biogas, a deoxygenation reactor (R-301, as a *RGibbs* model) is included upstream M − 202 mixer. This equipment removes the residual oxygen through controlled combustion with a minimal fraction of methane [64], reducing its concentration to values below 0.001 %^{v}.

For this project, thermocatalytic methanation was selected due to its greater technological maturity and industrial scalability compared to biological alternatives [65]. The catalyst used consists of a bimetallic active phase of nickel and iron with a 3:1 mass ratio, supported on a γ-Al_2O_3. The addition of a second metal (iron) has been shown to have positive effects on reaction performance compared to conventional nickel or ruthenium catalysts [11]. The kinetics employed follow those proposed by *Farsi* et al. [66] for a catalyst with the same characteristics and a metal loading of 17 %^{w}. The proposed reaction mechanism consists of two sequential steps, rWGS (r.2) and rSMR (r.3). The adjusted kinetic equations are based on a Langmuir-Hinshelwood-Hougen-Watson (LHHW) type model described in the above-mentioned reference [66]. Catalyst particles have a diameter of 5 mm and a sphericity of 1. The void fraction in the bed is supposed to be 0.5.

$$CO_{2\,(g)} + H_{2\,(g)} \rightleftharpoons CO_{(g)} + H_2O_{\,(g)} \quad ; \quad \Delta H^0_{rWGS} = +41.2\ \left[kJ{\cdot}mol^{-1}\right] \qquad \text{(r.2)}$$

$$CO_{(g)} + 3\,H_{2\,(g)} \rightleftharpoons CH_{4\,(g)} + H_2O_{\,(g)} \quad ; \quad \Delta H^0_{rSMR} = -206.3\ \left[kJ{\cdot}mol^{-1}\right] \qquad \text{(r.3)}$$

The methanation system includes two isothermal multitubular fixed-bed reactors (R-302 and R-303, Table 5) arranged in series, with intermediate condensation stages (T-301 and T-302) for water removal.

This configuration favors thermodynamic conversion by shifting the equilibrium towards methane formation. The reactors have been simulated using *RPlug* block, based on a 1D pseudo-homogeneous design. The model assumes that the bed is uniformly distributed along the reactor without incurring intra- or interparticle concentration gradients (absence of control by external and internal diffusion). It is also assumed that the radial dispersion of species is negligible, and that the concentration progression remains constant along the axial direction. In its resolution, *Aspen Plus*® employs the integral method to solve the mass and energy conservation equations for each differential reactor length element. The pressure losses caused by gas flow through the packed bed of catalyst particles are determined using the *Ergun* equation. The operating conditions are adjusted to the most favorable thermodynamic limit values (Figs. 2 and 3 -both graphs were performed using an *RGibbs* reactor in *Aspen Plus*®, with the *PR-BM* fluid package), with which the experimental kinetics were determined (18 bar, 300 °C), to maximize CO_2 conversion and minimize the formation of secondary products such as carbon monoxide (CO).

The reactors have a configuration similar to shell-and-tube heat exchangers, with a cooling system that uses pressurized water, which

Table 4
Electrolyzer characteristics.

Property	Unit	Value
Water consumption	kg/h	1160
Voltage	V	185
Current	A	34,500
Power	MW	6.4
Stacks	adim.	6
Efficiency HHV	%	80
Efficiency LHV	%	70
Temperature	°C	50
Pressure	bar	10
Electrolyte concentration	%^{w}	25
H_2 Purity	%^{v}	100

Table 5
Features of the methanation reactors.

Feature	Unidad	R-302	R-303
Length	m	2.44 (8 ft)	
No. of tubes	adim.	150	
Tube diameter	cm	1.91 (3/4 in)	
Volume	m^3	0.185	
Temperature	°C	300	
Particle diameter, d_p	mm	5	
Void fraction, ε	adim.	0.5	
Sphericity, Φ	adim.	1	
Pressure	bar	≈18	≈17
ΔP (Ergun)	bar	0.5	0.2
GHSV	h^{-1}	4600	2800
CO_2 conversion, (x_{CO2})	%	83.15	81.10
CH_4 fraction (at exit), (y_{CH4})	%^{v}	73.55	91.32

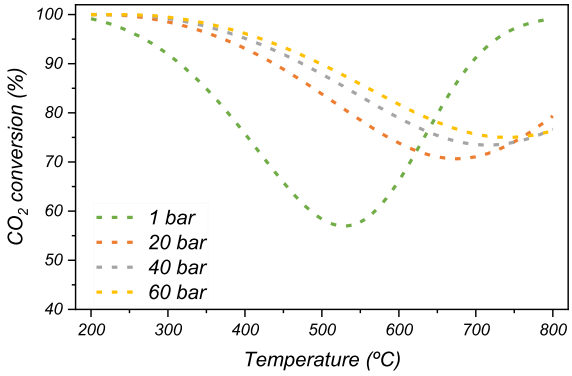

Fig. 2. Effect of temperature and pressure on CO_2 conversion in thermodynamic equilibrium. Calculated by minimization of Gibbs free energy.

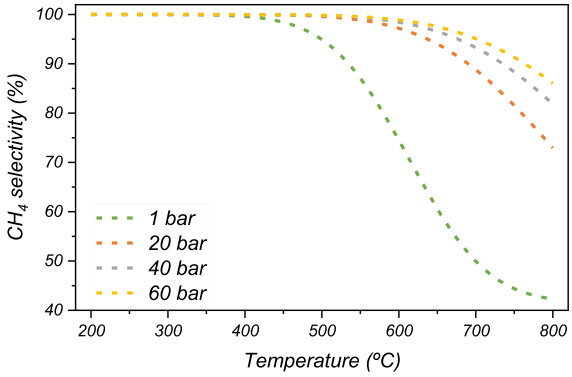

Fig. 3. Effect of Temperature and Pressure on CH_4 selectivity in thermodynamic equilibrium. Calculated by minimization of Gibbs free energy.

evaporates by absorbing the heat released during the exothermic reaction. The generated high-pressure steam (250 °C, ≈40 bar) can subsequently be utilized as a heat source or for power generation within the plant. The main characteristics, such as tube diameter, length, and catalyst particle size, were optimized to minimize pressure losses and ensure high process efficiency.

3.4. Dehydration

The *Sabatier* reaction (r.1) not only produces methane but also generates water as a byproduct (r.1). In order to ensure safety processing and transportation of natural gas, Spanish gas regulations [44] limit the water content setting a dew point of 2 °C at 70 bar. This is equivalent to 100 ppm, under standard conditions, as outlined in the Supplementary Material. To achieve that goal, different dehydration technologies were evaluated, including adsorption, refrigeration, and chemical absorption using glycols [67]. Chemical absorption with triethylene glycol (TEG) was selected as the most suitable option due to its widespread use in the gas industry, high efficiency in water removal, and ease of solvent regeneration at near-atmospheric pressures [68]. Additionally, TEG presents significant advantages over other glycols, such as diethylene glycol (DEG) or monoethylene glycol (MEG), thanks to its lower volatility, reduced vaporization losses, and greater thermal stability.

The dehydration process follows a topology similar to that of the desulfurization stage, utilizing an absorber (T-401) and a regenerator (T-402). Absorption and rectification columns (features detailed in Table 6) are simulated using *RadFrac* blocks configured with three sieve trays,

Table 6
Features of the dehydration section columns.

Property	Units	T-401	T-402
Number of trays	trays	3	3
Solution temperature (inlet)	°C	40	165
Operating temperature	°C	36.7–35.9	142–204.0
Operating pressure	bar	39.9–40	142.7–154.4
Tray spacing	m	0.6096	0.6096
Internal diameter	m	0.146	0.1437
Tray type	–	Sieve	Sieve
Tray height	m	1.82	1.83
Total height	m	2.30	2.31
% Flooding	–	80	80

spaced 24 inches (0.61 m) apart, and an internal diameter of approximately 0.15 m. The pressure drop per tray is estimated in 0.7 kPa, while the assumed efficiency is 100 %. TEG, with an initial purity of 99 %^{w}, enters the absorber at a temperature of 40 °C, where it removes moisture from the SNG until water concentrations fall below 93 ppm. After this stage, the enriched glycol is preheated through a heat exchanger (E-402) before entering the regenerator (T-402), which operates at a pressure of approximately 1 bar and temperatures below 204 °C -the critical limit to prevent solvent degradation- [69]. To enhance the efficiency of the regenerator, a low-pressure stripping air stream is used to reduce the water vapor pressure in the glycol solution, allowing the regenerated TEG to reach a purity of 99 %^{w} [70].

3.5. Cogeneration

A cogeneration plant has been incorporated into the facility to improve efficiency and gain energy independence, utilizing part of the desulfurized biogas to simultaneously produce electricity and heat. The cogeneration system consists of an open-cycle gas turbine configuration, converting the chemical energy of the biogas into electrical and thermal energy. This cycle comprises four main stages: air compression (multistage compression: C-502, C-503 and C-504 with intercoolers), constant pressure combustion (R-501) (up to 1000 °C), expansion in the turbine (TG-501), and exhaust gas release. Since the energy released by the reactors is insufficient to meet the facility's thermal demands, an auxiliary boiler (E-504) is incorporated to generate steam under the same conditions as previously mentioned. The boiler utilizes the exhaust gases from the turbine, which remain hot (450 °C). After passing through the boiler, the gases flow through a regenerator (E-503), designed to preheat the compressed air before combustion, reducing fuel consumption.

Sweetened biogas was selected as the fuel due to its low H_2S content, which reduces equipment corrosion and minimizes atmospheric pollutant emissions. The cycle's compression ratio was adjusted to an optimal value of 12, achieving a balance between thermal efficiency, slightly exceeding 30 %, and network output. Although the cycle exhibits a back-work ratio of 55 % (due to the compressor's high energy demand), integrating the regenerator and optimizing the system's design mitigate these losses and enhance overall performance. The isentropic efficiencies of the compression train and turbine, along with the pressure losses in the heat exchangers, were included in the system performance calculations.

3.6. Economic analysis

The economic analysis conducted for this biogas upgrading plant is based on an "estimated" or "factored" approach, using the costs of the main equipment as a basis to determine the total capital investment. Although this method, widely used in preliminary studies, has an error margin of ±20–30 %, it provides reasonable results with limited technical information [71]. Additionally, this methodology simplifies the calculation process by avoiding the use of advanced tools such as the

Aspen Process Economic Analyzer (APEA), which, although more precise, functions as a "black box" with non-transparent algorithms for the user.

The *Capital Expenditure* (CAPEX) includes the *Total Capital Investment* (C_{TCI}) required for the design, construction, and commissioning of the plant. In this case, CAPEX is broken down into *Total Permanent Investment* (C_{TPI}) and *Working Capital* (C_{WC}). C_{TPI} comprises fixed assets such as equipment and buildings, while C_{WC} covers initial operating costs, including inventory and accounts receivable funds.

The costs associated with each CAPEX component (Table 7), such as site preparation, auxiliary service installation, or unforeseen contingencies, were calculated by applying proportional corrections to the total cost of the main equipment or *Total Bare-Module* cost (C_{TBM}), following the factorization proposed by *Busche* [72]. The C_{TBM} represents the sum of the *Bare-Module* costs (C_{BM}, eq. (1)) for each major item of process equipment (e.g., fabricated vessels, compressors, pumps …). To determine each C_{BM}, base cost (C_B) must be first estimated, which corresponds to a standard design (near-ambient pressure, carbon-steel material …) for a given capacity, as per correlations in *Seider* et al. [71]. Adjustments for actual pressure, materials, and design complexity yield the purchase cost (C_P). Comprehensive details regarding these factors are included in the Supplementary Material for each type of equipment. Next, module factors from *Guthrie* [73] are applied to C_P to account for the indirect expenses of installing and integrating the equipment (e.g., foundation, support structures, instrumentation, insulation, electrical system …). Finally, the obtained cost is updated to the 2023 *Chemical Engineering Plant Cost Index* (CEPCI) and the corresponding currency exchange rate (USD to EUR), as 2023 provides the most recent consolidated data available for accurate cost estimation. New reports for 2024 are expected to be released during the first semester of 2025. Note that in (eq. (1)), cost index $CEPCI_{XXXX}$ corresponds to the year (XXXX) that applies to the purchase cost.

$$C_{BM} = C_P \cdot F_{BM} \cdot \frac{CEPCI_{2023}}{CEPCI_{XXXX}} \cdot \frac{€_{2023}}{USD_{2023}} \quad (1)$$

The total operating costs (Table 8), also known as *Operational Expenditures* (OPEX), can be divided, according to *Seider* et al. [71], as the sum of production costs (*COM -Cost of Manufacture*-direct expenses including raw materials, utility streams, labor and maintenance costs, plant operating expenses, insurance, depreciation, and taxes-) and general expenses (*GE -Total General Expenses*-covering administrative costs, research and development, management, and commercial services-). These expenses are calculated based on projected annual sales. Raw materials are acquired in industrial quantities, assuming constant prices under long-term contracts. Some factors include the reference source consulted to establish the base price.

Table 7
CAPEX factors [72].

Factor	Description
Equipment purchase, C_{TBM}	Initial value
Site preparation cost, C_{site}	5 % C_{TBM}
Utility installation cost, C_{serv}	1.5 % C_{TBM}
Cost allocated to auxiliary and related installations, C_{alloc}	Cooling circuit
Direct permanent investment, C_{DPI}	Sum of C_{TBM}, C_{site}, C_{serv}, and C_{alloc}
Contingency costs and contractor fees, C_{cont}	35 % C_{DPI}
Total depreciable capital, C_{TDC}	Sum of C_{DPI} and C_{cont}
Land cost, C_{land}	2 % C_{TDC}
Licensing costs, C_{royal}	2 % C_{TDC}
Startup cost, $C_{startup}$	10 % C_{TDC}
Total permanent investment, C_{TPI}	Sum of C_{TDC}, C_{land}, C_{royal}, and $C_{startup}$
Working capital, C_{WC}	15 % C_{TPI} or a lower estimate
Total capital investment, C_{TCI}	Sum of C_{TPI} and C_{WC}

Table 8
OPEX factors.

Factor	Description
Raw Materials	
Process water	0.75 USD/1000 US gal [71]
MDEA	1.45 USD/kg [74]
KOH	0.67 USD/kg [75]
TEG	0.55 USD/kg [74]
Catalyst	2.2 USD/kg [76]
Utilities	
Electricity	100.20 €/MWh [77]
Labor Costs (O)	
Direct Wages and Benefits (DW&B)	2360 €/operator [78]
Salaries and direct benefits (for supervisors and engineers)	15 % DW&B
Supplies and operational services	6 % DW&B
Technical assistance	60,000 USD/(operator/shift) · yr//2 operators per shift
Laboratory control	65,000 USD/(operator/shift) · yr//2 operators per shift
Maintenance Costs (M)	
Maintenance Wages and Benefits (MW&B)	3.5 % C_{TDC}
Salaries and direct benefits	25 % MW&B
Materials and services	100 % MW&B
Preventive maintenance	5 % MW&B
General Operating Expenses (from Combined Salary, Wages, and Benefits for Maintenance and Labor-related Operations, M&O-SW&B)	
General plant expenses	7.1 % M&O-SW&B
Mechanical services department	2.4 % M&O-SW&B
Human Resources department	5.9 % M&O-SW&B
Commercial services	7.4 % M&O-SW&B
Property Taxes and Insurance	
Total	2 % C_{TDC}
Depreciation	
Direct plant	5 % C_{TDC}
Auxiliary plants	6 % de 1.18 C_{alloc}
Costs of Manufacture (COM)	Sum of the above
Total General Expenses (GE)	
Sales expenses	3 % of sales
Research expenses	4.8 % of sales
Auxiliary research	0.5 % of sales
Administrative expenses	2 % of sales
Management compensation	1.25 % of sales
Total General Expenses (GE)	Sum of the above
Total Production Costs	COM + GE

4. Results and discussion

4.1. Gas quality and sale

The synthetic natural gas generated in the plant has a flow rate of 1098.71 Nm^3/h, equivalent to 8790×10^6 Nm^3/year. Table 9 details the gas properties after the final treatment stage, which comply with the requirements established by Spanish gas legislation [44]. The obtained values lie within the limits set by the regulatory framework, thereby guaranteeing the viability of the SNG for injection into the gas grid. Also, in Table 9 has been included the properties of the raw biogas for comparative purposes.

Additionally, gases from non-conventional sources are subjected to extra requirements, mainly related to their composition [45]. Again, the gas meets these requirements, although a small percentage of CO_2 and unreacted H_2 is observed. Table 10 details the final composition of SNG compared to that of raw biogas.

The annual revenue from gas sales is based on the average “spot”

Table 9
Quality of the raw biogas, the synthetic natural gas (SNG) produced, and regulated limits (Min & Max) for comparison purposes.

Property (*)	Units	Raw Biogas	SNG	Min.	Max.
Wobbe Index	kWh/m^3	6.116	13.811	13.403	16.058
Higher heating value (HHV)	kWh/m^3	6.061	10.32	10.26	13.26
Relative Density	–	0.9819	0.558	0.555	0.700
Total Sulfur (excluding odorant)	mg/m^3	1430	0.33	N/A	50
O_2	mol/mol	0.7 %	0	N/A	0.001 %
CO_2	mol/mol	42 %	1.05 %	N/A	2.5 %
Water Dew Point (°C at 70 bar (a))	°C	–	+1.0	N/A	+2

(*) Properties are expressed under standardized reference conditions: [0 °C; V(0 °C; 1.01325 bar)].

Table 10
Composition of the raw biogas and the synthetic natural gas produced.

Species	Units	Raw Biogas	SNG	Min.	Max.
CH_4	mol %	54.5 %	91.72 %	90 %	N/A
CO	mol %	–	0.01 %	N/A	2 %
H_2	mol %	–	4.2 %	N/A	5 %

price for 2023 in the *Iberian Gas Market* (MIBGAS), the primary platform for trading these products. In this market, different natural gas products are traded, each related to the delivery period or type of delivery. For instance, the daily product D+1 corresponds to gas purchased for next-day delivery, while the monthly product M+1 covers contracts for gas supply in the following month. There is also same-day delivery (intraday product), quarterly delivery (Q+1) and annual delivery (Y+1).

The 2023 fiscal year began with the D+1 and M+1 products priced at 70 €/MWh; thereafter, prices gradually declined, ending the year at around 30 €/MWh. The representative annual average traded on MIBGAS for the D+1 product (which is usually like M+1) was 39.11 €/MWh (compared to 99.16 €/MWh in 2022) [79]. By using the synthetic natural gas HHV, expressed in MWh/Nm^3, the normal flow rate (at 1 atm; 273 K) produced by the plant, and the annual operating hours (8000 h/year), the annual revenue from injection is determined (see Table 11).

4.2. CAPEX

Table 12 shows the distribution of the *Bare Module* costs according to equipment type. The most significant expenditures, ranked from highest to lowest, are associated with the electrolyzer, the turbine, the columns (including trays, condensers, and boilers), and compressors. Notably, more than 30 % of the equipment costs are attributed to the compression and expansion stages, which are dedicated to adjusting stream pressures and, in the case of the turbine, generating electricity. Conversely, the reactors, which constitute the core of the installation, account for a relatively small percentage (2.38 %) of the total costs. This is largely because the methanation reactor design operates at moderate pressures (~18 bar) and standard temperatures (~300 °C), which allow the use of fairly conventional shell-and-tube vessels without exotic alloys or special configurations.

Table 13 shows the distribution of costs by plant sections, as also illustrated in Fig. 4. As anticipated by Table 12, the highest budgets are allocated to the cogeneration and electrolysis sections (which contain the most expensive devices), whereas methanation has a much smaller impact in conjunction with dehydration. The pretreatment zone, or desulfurization, exhibits an intermediate impact between these sections.

These results prompt a reflection on key design aspects and open the way for future scenarios. The high costs associated with cogeneration raise doubts about its profitability in the current design. A viable alternative could be the implementation of an auxiliary boiler to meet high-pressure steam requirements for heating, purchasing electricity from the grid rather than generating it internally. Conversely, although electrolysis is a key technology in this process, it remains quite expensive. It is foreseeable though, that in the years to come the costs associated with hydrogen production will decrease and stabilize, thereby improving its economic viability.

Furthermore, Table 14 shows the total capital investment required for the installation, with a final cost of 21.83 million euros. Except for the costs associated with the refrigeration circuit and working capital, which can be estimated using *Seider* et al. equations [71], the remaining items are calculated as a fraction of the C_{TBM}.

Table 11
Revenue generated from SNG.

Yearly average flowrate, (Nm^3/h)	1098.71
$HHV_{SNG\ (in\ normal\ conditions)}$, MWh/Nm^3	0.01032
Natural gas "spot" price, 2023 (€/MWh)	39.11
Revenue, 2023 (M€/year)	3.550

4.3. OPEX

Overall, OPEX amounts to 7.776.235,79 € per year (Table 15), with manufacturing costs (COM, see Table 8) accounting for approximately 91 % of the total OPEX. Within this large share, electricity consumption stands out as the major component of the installation's operating expenses. The electrolysis stage requires approximately 86 % of the plant's total electricity, reflecting its significant impact on energy costs. Although it is considered that electrolysis could be partially powered by renewable sources during favorable hours, the limited coverage of these sources in the Spanish grid implies that a substantial portion of the electricity will be sourced from the grid, with prices varying according to demand and available generation (averaging 100.2 €/MWh). With an annual expenditure of 3.2 M€ on electricity plus raw materials, the project's gross margin (revenues minus supply costs) is reduced to 270,000 €/year. Additionally, maintenance and depreciation (assuming a useful life of 20 years with linear depreciation at 5 % per year), both linked to the C_{TDC} (and thus to CAPEX), involve similar total costs of

Table 12
Distribution of the Bare Module Cost (C_{TBM}) by equipment type.

Function	C_{TBM} (€, 2023)	% C_{TBM}
Compressors and Electric Motors	1,605,193.13	12.69
Pumps	91,114.54	0.72
Heat Exchangers	844,886.37	6.68
Reactors	301,368.15	2.38
Columns	2,307,856.55	18.25
Turbine	3,231,161.27	25.55
Hydrogen Tank	577,130.66	4.56
Electrolyzer	3,689,030.23	29.17

Table 13
Distribution of C_{TBM} by plant sections.

Zone	C_{TBM} (€, 2023)	% C_{TBM}
Desulfurization	1,869,010.52	14.78
Methanation	831,085.85	6.57
Cogeneration	4,502,335.80	35.60
Electrolysis	4,874,632.83	38.51
Dehydration	575,169.07	4.55

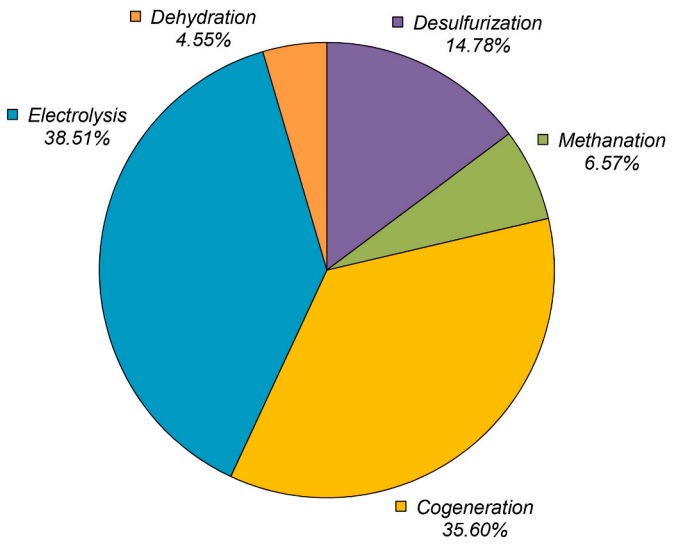

Fig. 4. Distribution of costs by plant sections.

Table 14
Distribution of CAPEX costs.

Factor	Cost (M€, 2023)	% C_{TCI}
Equipment Purchase, C_{TBM}	12.65	57.9
Permanent Direct Investment, C_{DPI}	13.59	62.3
Total Depreciable Capital, C_{TDC}	18.35	84.1
Total Permanent Investment, C_{TPI}	20.92	95.8
Working Capital, C_{WC}	0.91	4.2
Total Capital Investment, C_{TCI}	21.83	100.0

Table 15
Operational expenses (OPEX).

Factor	Cost (€/year, 2023)	Percentage (%)
Raw Materials	65,229.87	0.8
Services	3,214,435.54	41.3
Labor Costs (O)	568,661.48	7.3
Maintenance Costs (M)	1,476,996.99	19.0
General Operating Expenses	208,957.12	2.7
Property Taxes and Insurance	366,955.77	4.7
Depreciation	1,464,964.89	18.8
Production Costs (COM)	7,366,201.33	94.7
Total General Expenses (GE)	410,034.46	5.3
Total Production Expenses (COM + GE)	7,776,235.79	100

approximately 1.5 M€ each. This relationship ties the operating cost to the initial plant design and the total value of the investments required for construction and equipment. Although labor costs are more moderate compared to the aforementioned items, they still represent a significant expense of nearly half a million euros. When all these costs are subtracted from the previously reported gross margin, the result is a highly negative EBITDA (*Earnings Before Interest, Taxes, Depreciation, and Amortization*), a metric commonly used in income statements because it closely resembles operating cash flow -that is, the money generated by the investments through regular activities-.

The general expenses, which constitute the remaining 9 % of OPEX, include activities related to administration, research and development, safety, commercial services, and infrastructure maintenance. These items are estimated as a proportion of the sales generated, in line with typical industry values.

4.4. Economic viability

When marketing an alternative product to a resource as commonplace as natural gas, it is advisable to set a sale price that allows for a meaningful comparison between the two options. A practical method for determining this price is to base it on an expected *return on investment* (ROI) that ensures a specific objective is met (eq. (2)). For this calculation, it is essential to consider the applicable tax rate (t), which in this case has been assumed to be 40 % in light of the current fiscal framework in Spain.

$$ROI = \frac{Net\ Profits}{TCI} = \frac{(1-t)\cdot(Revenues - OPEX)}{C_{TCI}} \quad (2)$$

The high operating expenses estimated result in a considerably high profitability threshold (0 % ROI) for synthetic natural gas, at 91.75 €/MWh. This cost makes it unfeasible to compete with the average natural gas price in Spain along 2023 (39.11 €/MWh). This outcome, obtained for the base case of the installation (Scenario 1), underscores the need to explore alternatives that reduce the required investment. In this context, two potential cost-reduction strategies are proposed:

First Alternative (Scenario 2)**:** Eliminate the cogeneration section from the original design. This would imply that the supply of high-pressure steam and electricity must be sourced externally. Electricity would be purchased from the grid, while steam could be generated using a boiler fueled by a small fraction of the available biogas. To estimate the costs associated with this auxiliary installation, a correlation proposed by *Seider* et al. [71] based on the process steam requirements is used. Notably, the heat generated by the *Sabatier* reaction (r.1) is utilized to help produce the necessary steam, thereby optimizing the system's thermal efficiency.

Second Alternative (Scenario 3)**:** Eliminate both cogeneration and electrolysis, which entails the additional requirement to incorporate hydrogen into the system. This service has an official price in Spain set by MIBGAS at 5.85 €/kg [80], introducing a new economic variable into the analysis.

The results of the proposed alternatives, detailed in Table 16, reveal significant differences in key economic indicators. In both strategies, CAPEX is considerably reduced by eliminating the most expensive equipment from the base case (such as the turbine in cogeneration and the electrolyzer in electrolysis). This is particularly interesting given that fixed capital is often financed through debt, facilitating access to financial resources. However, the operational costs (OPEX) vary more complexly. The second scenario achieves the lowest OPEX (6.74 $M€_{2023}$/MWh) despite a higher electricity requirement, owing to the reduction in tangible capital and consequent decreases in costs related to amortization, insurance, and maintenance. In contrast, in the third scenario

Table 16
Economic feasibility of the different scenarios.

	Scenario 1	Scenario 2	Scenario 3
CAPEX ($M€_{2023}$/MWh)	21.83	13.62	5.61
OPEX ($M€_{2023}$/MWh)	7.78	6.74	9.24
0 % Profitability Threshold ($€_{2023}$/MWh)	91.75	79.54	108.95
20 % Profitability Threshold ($€_{2023}$/MWh)	187.02	135.30	131.93

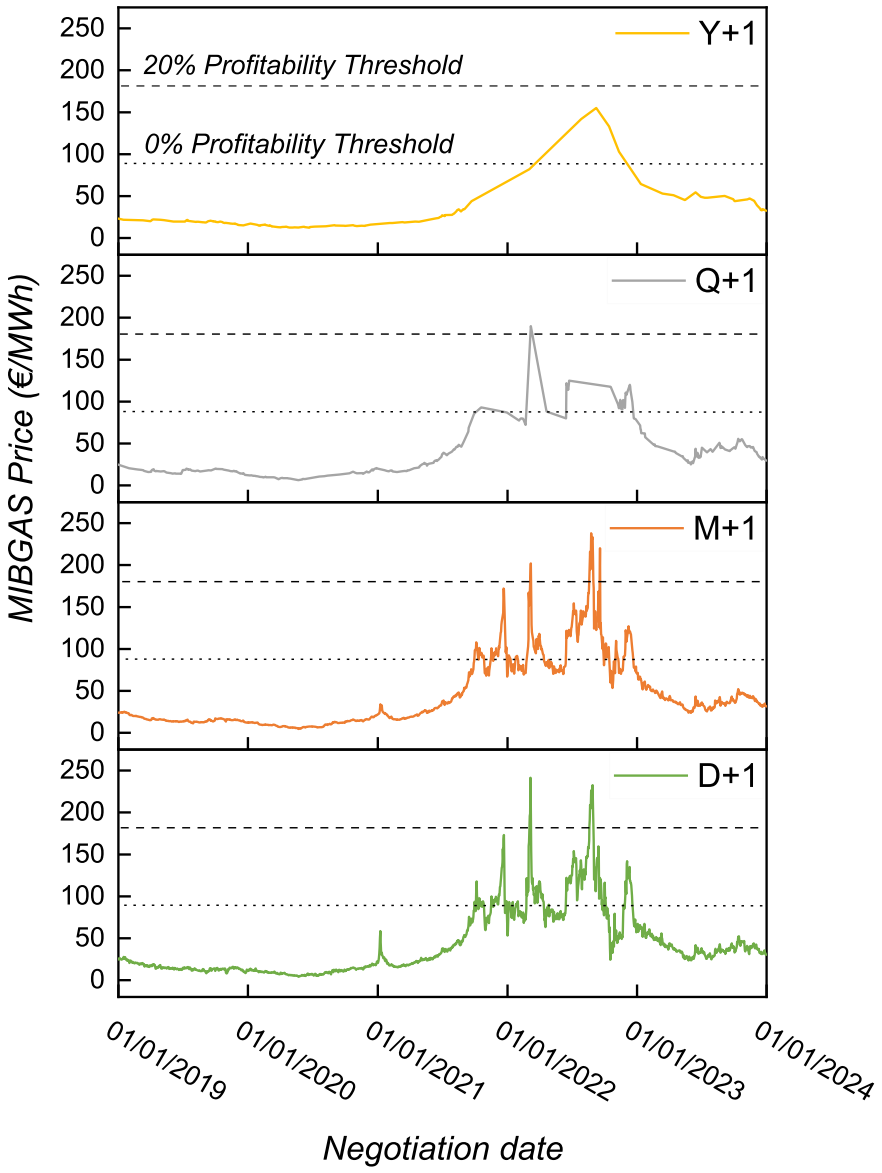

Fig. 5. Evolution of the MIBGAS product prices for the period 2019–2024 and the threshold of profitability [81].

(9.24 M€$_{2023}$/MWh), the increase in OPEX is explained by the price of hydrogen, which offsets the savings from a lower depreciable capital.

The break-even thresholds (for a 0 % and a 20 % ROI, as defined in eq. (2)) also show marked differences between the scenarios. The first scenario requires the highest price for synthetic natural gas to achieve a 20 % profitability threshold (187.02 €/MWh). In contrast, the third scenario exhibits the lowest 20 % profitability threshold (131.93 €/MWh) but also sets the highest price needed to obtain a positive return (108.95 €/MWh). Finally, the second scenario emerges as the most balanced alternative, with the lowest 0 % profitability threshold (79.54 €/MWh) and a competitive 20 % value (135.30 €/MWh) compared to Scenario 3.

Fig. 5 illustrates the price trends of MIBGAS products (D+1, M+1, Q+1 and Y+1) between 2019 and 2024 [81] and profitability thresholds of Scenario 1. A sharp price increase is evident between late 2021 and mid-2022, likely driven by external factors such geopolitical tensions, supply chain disruptions and energy market volatility in Europe. This spike notably surpasses the 0 % profitability threshold, particularly for the M+1 and D+1 products. Outside this interval, prices remain relatively stable and below the profitability thresholds, suggesting limited incentives under baseline conditions. The Y+1 and Q+1 products exhibit less pronounced fluctuations, indicating more stability in longer-term contracts compared to the high volatility seen in shorter-term (D+1 and M+1) markets.

4.5. Forecast scenario for 2030

As in other studies [82,83], the main limiting factors in the plant's cost structure are electricity in the OPEX and hydrogen production (Electrolyzer) in the purchased equipment. Considering these factors are expected to decrease significantly in next year's [84–86], this study proposes an estimation of the projected profitability thresholds for synthetic natural gas (SNG) pricing by 2030 doing a bidimensional analysis of different variables. In Scenarios 1 and 2, the key variables to be assessed include electricity prices and the cost of alkaline electrolyzers, which not only impact capital expenditure (CAPEX) but also

influence operational costs through maintenance, insurances, and depreciation (see Table 7). Conversely, Scenario 3 will be determined by the evolution of both electricity and hydrogen prices in the Spanish market.

The estimated electricity price for this horizon has been derived from the *National Integrated Energy and Climate Plan* (PNIEC 2023–2030) [87], which sets a variable electricity cost in the Spanish market in 2030 within the range of 29.8–36.6 €/MWh, representing a substantial reduction compared to current values. In line with this trend, a significant reduction in electrolyzer costs is also projected. According to *Krishnan* et al. [88], price of alkaline *stacks* is expected to decrease from the current range of 242–388 €/kW to an estimated 52–79 €/kW by 2030, thereby improving the competitiveness of electrolysis as a hydrogen production technology. Consequently, hydrogen prices will also be affected by these cost reductions, as their production is directly linked to electricity prices and electrolysis technology optimization. According to the *Net Zero Emissions by 2050* scenario, hydrogen costs are expected to range between 2 and 9 € per kg of H_2 by 2030 (obtained by renewable sources), driven by infrastructure development and economies of scale [6]. However, the current price of hydrogen in Spain (5.85 €/kg) is considerably lower than the upper limit established by that estimation. For that reason, the price has been set at a maximum of 5 €/kg. It is important to highlight that these values fall within a historic context of energy transition and the promotion of low-carbon technologies, where cost reductions play a crucial role in ensuring the economic feasibility of both hydrogen and SNG in a sustainable energy system. The price ranges mentioned delineate two possible outlooks (Table 17): an optimistic one, based on the most favorable estimates; and a pessimistic projection, within the framework of economic and technological uncertainty associated with the sector's development.

Results for different outlooks and scenarios are shown in Fig. 6. The detailed bidimensional analysis reveals improvements in economic viability; however, the trends remain consistent with those of the base case. The most favorable conditions (29.8 €/MWh electricity, 52 €/kW electrolyzers, and 2 €/kg hydrogen) reduce breakeven prices by 30–50 % across all scenarios. Scenario 2 emerges as the most economically robust configuration, maintaining viable profitability thresholds between 38.77 and 78.09 €/MWh across both favorable and unfavorable conditions. This resilience suggests the potential advantage of incorporating an owned electrolyzer in the facility and the benefits achieved by using a more affordable electrical supply. In contrast, Scenario 1 demonstrates significantly higher breakeven points (53.21–128.96 €/MWh), with a similar variability depending on key parameters. The cost increase over Scenario 2 baseline indicates the same structural cost challenges, potentially from capital-intensive cogeneration requirements or suboptimal energy conversion efficiencies seen in the base case. Finally, Scenario 3 presents a unique risk profile, where its intermediate performance under baseline conditions (50.89–73.87 €/MWh) deteriorates dramatically when hydrogen prices increase. The cost escalation triggered by H_2 price movements from 2 to 5 €/kg highlights this configuration's acute exposure to hydrogen market volatility. This suggests that while Scenario 3 design may offer theoretical advantages due to less capital expenditure, its practical implementation would require either secured hydrogen supply contracts to mitigate price risks, or technological breakthroughs to reduce hydrogen production prices even more.

By the year 2030, a shift in SNG prices is also anticipated. The PNIEC plan [87] projects a natural gas cost of 28.5 €/MWh in Spain, which is more similar to the average cost of 22 €/MWh before the energy crisis.

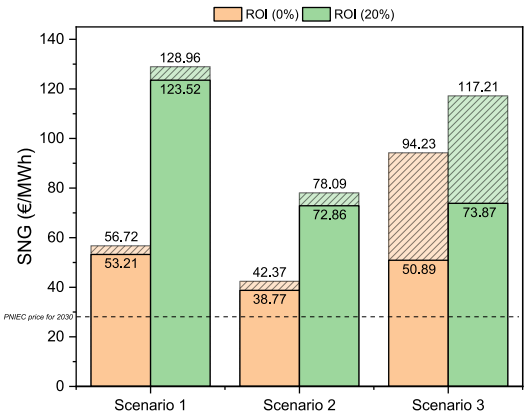

Fig. 6. Minimum required SNG price for profitability (€/MWh). Solid bars: Favorable pattern; Striped bars: Unfavorable pattern; PNIEC Natural Gas price forecast for 2030 = 28.5 €/MWh [87].

This cost estimate renders the project more financially viable and affordable. It is important to acknowledge that this analysis has not incorporated the consideration of funds or carbon tax revenues. Consequently, the cost projections may exhibit enhanced accuracy if these factors are considered.

5. Conclusions

Technically, all the evaluated technologies are suitable for executing the process and achieving the intended goal - a synthetic natural gas with sufficient quality to be marketed within the gas industry. However, the economic evaluation of the installation, with a 1100 Nm^3/h SNG capacity, has highlighted several factors that affect its viability. Electrolysis, despite being a key technology in the process, remains expensive both in terms of initial investment and operational costs; approximately one-third of the plant's CAPEX and OPEX are attributable to this section. Cogeneration, while significantly reducing operational expenses and offering the advantage of operating as an "energy island," also requires a considerable investment, with the compression and expansion stages accounting for up to 38 % of the total equipment cost. Based on these findings, two alternative scenarios (labelled as 2nd and 3rd scenario) were proposed: one that eliminates the cogeneration section, and another that omits both cogeneration and electrolysis.

In the second scenario, the removal of cogeneration significantly reduces both CAPEX and OPEX. Purchasing electricity from the grid and generating steam via a boiler fueled by sweetened biogas are identified as technical and economically viable alternatives. However, reliance on grid electricity presents a future challenge in terms of cost stability, so maximizing the use of renewable energy is recommended to mitigate this uncertainty.

With the third scenario, eliminating both electrolysis and cogeneration results in a simpler configuration but incurs higher operating costs, primarily due to the price of purchased hydrogen. Although this scenario presents the lowest 20 % profitability threshold among those analyzed, it also sets the highest price required for economic viability, which could limit its competitiveness.

Table 17
Input parameters for bidimensional analysis.

Outlook	Electricity Price (€/MWh)	Electrolyzer stack (€/kW)	H_2 Price (€/kg)
Favorable conditions	29.8	52	2
Unfavorable conditions	36.6	79	5

A particularly notable aspect of the analysis is the low cost associated with methanation technology, which constitutes the "core" of the SNG production process. Nevertheless, the use of catalytic methanation imposes additional requirements on other stages—such as desulfurization, which must reduce H_2S concentrations to extremely low levels (0.1 ppm), and the effective removal of the water produced. These measures are crucial to ensuring the quality of synthetic natural gas and its suitability for injection into the gas grid. With the current plant design and natural gas pricing, the investment is not economically viable -although it is technically feasible-. If the natural gas price were to reach 200 €/MWh, an acceptable 20 % return could be achieved. However, such conditions have only been observed under anomalous, short-term circumstances (e.g., throughout the year 2022, driven by geopolitical conflicts, the price of natural gas in Spain reached levels of up to 240 €/MWh [89]), limiting the long-term sustainability of this approach.

A study of new trends in key variables by 2030 reveals the potential for enhanced profitability. The analysis, which focuses on electricity prices (29.8–36.6 €/MWh) [87], electrolyzer costs (52–79 €/kW) [88], and hydrogen prices (2–5 €/kg) [6], indicates that a reduction in these costs could lead to an improvement in profitability thresholds. All scenarios demonstrate an improvement in their profit margins, with Scenario 2 (removal of cogeneration zone) breakeven price potentially reaching 38.77 €/MWh under optimal conditions. However, even under these favorable circumstances, they cannot approach fossil natural gas prices to achieve true competitiveness. For investors and policymakers, this underscores the importance of continued technological advancement and market conditions in realizing competitive SNG production. Consequently, optimizing critical technologies and diversifying energy sources are essential strategies to enhance the competitiveness of the plant in the future. Beyond the techno-economic considerations of the produced SNG, the environmental benefits of reducing fossil fuel consumption and utilizing a waste stream should also be noted, as these aspects could be translated into economic terms in the situation of new sustainability policies.

CRediT authorship contribution statement

P. Sanz-Monreal: Writing – original draft, Visualization, Software, Formal analysis, Conceptualization. **V.D. Mercader:** Writing – review & editing, Supervision, Investigation, Formal analysis, Conceptualization. **P. Aragüés-Aldea:** Data curation, Conceptualization. **P. Durán:** Validation, Resources, Investigation, Data curation. **E. Francés:** Visualization, Formal analysis, Conceptualization. **J. Herguido:** Writing – review & editing, Validation, Formal analysis, Conceptualization. **J.A. Peña:** Writing – review & editing, Validation, Supervision, Project administration, Funding acquisition, Conceptualization.

Acknowledgements

This research has been funded by MICINN (*Spanish Ministerio de Ciencia e Innovación*), Agencia Estatal de Investigación (AEI) project number PID2022-136947OB-I00 and European Union Next Generation PRTR-C17.I1 Task LA4.A1. Additionally, the consolidated research group *Catalysis and Reactor Engineering Group* (CREG) (T43-23R) has received financial support from *Gobierno de Aragón* (Aragón, Spain) through the European Social Fund – FEDER.

In addition, P. Aragüés-Aldea and V. D. Mercader (grant no. PRE2020-095679) express their gratitude for the research predoctoral grants of *Gobierno de Aragón* and Spanish *Ministerio de Ciencia e Innovación* respectively.

Lastly, authors also acknowledge the work of *Servicio General de Apoyo a la Investigación-SAI* (Universidad de Zaragoza).

Appendix A. Supplementary data

Supplementary data to this article can be found online at https://doi.org/10.1016/j.biombioe.2025.107871.

Data availability

Supplementary data associated with this article can be found in the online version

References

[1] E.P. Olaguer, Greenhouse gas emissions and climate impacts, in: Atmospheric Impacts of the Oil and Gas Industry, Elsevier, 2017, pp. 55–64, https://doi.org/10.1016/B978-0-12-801883-5.00006-1.
[2] M. Shahzad Javed, J. Jurasz, T.H. Ruggles, I. Khan, T. Ma, Designing off-grid renewable energy systems for reliable and resilient operation under stochastic power supply outages, Energy Convers Manag 294 (2023) 117605, https://doi.org/10.1016/j.enconman.2023.117605.
[3] H. Hissou, S. Benkirane, A. Guezzaz, M. Azrour, A. Beni-Hssane, A novel machine learning approach for solar radiation estimation, Sustainability 15 (2023) 10609, https://doi.org/10.3390/su151310609.
[4] R. Shan, N. Kittner, Sector-specific strategies to increase green hydrogen adoption, Renew. Sustain. Energy Rev. 214 (2025), https://doi.org/10.1016/j.rser.2025.115491.
[5] A.K. Sarker, A.K. Azad, M.G. Rasul, A.T. Doppalapudi, Prospect of green hydrogen generation from hybrid renewable energy sources: a review, Energies (Basel) 16 (2023) 1556, https://doi.org/10.3390/en16031556.
[6] International Energy Agency (IEA), Global hydrogen review 2024 – analysis. https://www.iea.org/reports/global-hydrogen-review-2024, 2025.
[7] S. Ahmad, A. Ullah, A. Samreen, M. Qasim, K. Nawaz, W. Ahmad, A. Alnaser, A. M. Kannan, M. Egilmez, Hydrogen production, storage, transportation and utilization for energy sector: a current status review, J. Energy Storage 101 (2024), https://doi.org/10.1016/j.est.2024.113733.
[8] D. Martins, T. Cabrita, J. Rodrigues, J. Puna, J. Gomes, Utilisation of liquefied biomass in water Co-electrolysis for the production of synthesis gas, Energy. Storage. Appl. 2 (2025) 2, https://doi.org/10.3390/esa2010002.
[9] A. Gonçalves, J.F. Puna, L. Guerra, J.C. Rodrigues, J.F. Gomes, M.T. Santos, D. Alves, Towards the development of syngas/biomethane electrolytic production, using liquefied biomass and heterogeneous catalyst, Energies (Basel) 12 (2019), https://doi.org/10.3390/en12193787.
[10] P. Sabatier, J. Senderens, Nouvelles synthèses du méthane, C. R. Acad. Sci. Paris (1902) 514–516.
[11] A. Sanz-Martínez, P. Durán, V.D. Mercader, E. Francés, J.Á. Peña, J. Herguido, Biogas upgrading by CO_2 methanation with Ni-, Ni–Fe-, and Ru-based catalysts, Catalysts 12 (2022) 1609, https://doi.org/10.3390/catal12121609.
[12] K. Ghaib, F.Z. Ben-Fares, Power-to-Methane: a state-of-the-art review, Renew. Sustain. Energy Rev. 81 (2018) 433–446, https://doi.org/10.1016/j.rser.2017.08.004.
[13] J.R. Rostrup-Nielsen, K. Pedersen, J. Sehested, High temperature methanation: sintering and structure sensitivity, Appl. Catal. Gen. 330 (2007) 134–138, https://doi.org/10.1016/j.apcata.2007.07.015.
[14] P. Aragüés-Aldea, A. Sanz-Martínez, P. Durán, E. Francés, J.A. Peña, J. Herguido, Improving CO_2 methanation performance by distributed feeding in a Ni-Mn catalyst fixed bed reactor, Fuel 321 (2022), https://doi.org/10.1016/j.fuel.2022.124075.
[15] M. Saunois, A.R. Stavert, B. Poulter, P. Bousquet, J.G. Canadell, R.B. Jackson, P. A. Raymond, E.J. Dlugokencky, S. Houweling, P.K. Patra, P. Ciais, V.K. Arora, D. Bastviken, P. Bergamaschi, D.R. Blake, G. Brailsford, L. Bruhwiler, K.M. Carlson, M. Carrol, S. Castaldi, N. Chandra, C. Crevoisier, P.M. Crill, K. Covey, C.L. Curry, G. Etiope, C. Frankenberg, N. Gedney, M.I. Hegglin, L. Höglund-Isaksson, G. Hugelius, M. Ishizawa, A. Ito, G. Janssens-Maenhout, K.M. Jensen, F. Joos, T. Kleinen, P.B. Krummel, R.L. Langenfelds, G.G. Laruelle, L. Liu, T. Machida, S. Maksyutov, K.C. McDonald, J. McNorton, P.A. Miller, J.R. Melton, I. Morino, J. Müller, F. Murguia-Flores, V. Naik, Y. Niwa, S. Noce, S. O'Doherty, R.J. Parker, C. Peng, S. Peng, G.P. Peters, C. Prigent, R. Prinn, M. Ramonet, P. Regnier, W. J. Riley, J.A. Rosentreter, A. Segers, I.J. Simpson, H. Shi, S.J. Smith, L.P. Steele, B. F. Thornton, H. Tian, Y. Tohjima, F.N. Tubiello, A. Tsuruta, N. Viovy, A. Voulgarakis, T.S. Weber, M. van Weele, G.R. van der Werf, R.F. Weiss, D. Worthy, D. Wunch, Y. Yin, Y. Yoshida, W. Zhang, Z. Zhang, Y. Zhao, B. Zheng, Q. Zhu, Q. Zhu, Q. Zhuang, The global methane budget 2000–2017, Earth Syst. Sci. Data 12 (2020) 1561–1623, https://doi.org/10.5194/essd-12-1561-2020.
[16] D. Deublein, A. Steinhauser (Eds.), Biogas from Waste and Renewable Resources, Wiley, 2008, https://doi.org/10.1002/9783527621705.
[17] M. Noussan, V. Negro, M. Prussi, D. Chiaramonti, The potential role of biomethane for the decarbonization of transport: an analysis of 2030 scenarios in Italy, Appl. Energy 355 (2024) 122322, https://doi.org/10.1016/j.apenergy.2023.122322.
[18] V.D. Mercader, P. Aragüés-Aldea, P. Durán, E. Francés, J. Herguido, J.A. Peña, Optimizing sorption enhanced methanation (sem) of CO_2 with Ni_3Fe + lta 5 A mixtures, Catal. Today 453 (2025) 115262, https://doi.org/10.1016/j.cattod.2025.115262.
[19] V.D. Mercader, P. Durán, P. Aragüés-Aldea, E. Francés, J. Herguido, J.A. Peña, Biogas upgrading by intensified methanation (SESaR): reaction plus water adsorption - desorption cycles with Ni-Fe/Al_2O_3 catalyst and LTA 5A zeolite, Catal. Today 433 (2024) 114667, https://doi.org/10.1016/j.cattod.2024.114667.

[20] European Committee for Standardization (CEN), EN 16723-1:2016. Natural Gas and Biomethane for Use in Transport and Biomethane for Injection in the Natural Gas Network – Part 1: Specifications for Biomethane for Injection in the Natural Gas Network, 2016.
[21] European Committee for Standardization (CEN), EN 16726:2015+A1:2018. Gas Infrastructure – Quality of Gas – Group H, 2018.
[22] European Biogas Association (EBA), Variations in national regulations with respect to biomethane grid connection. https://www.europeanbiogas.eu/wp-content/uploads/2024/02/GreenMeUp-Variations-in-Natl.-Grid-Connection.pdf, 2024.
[23] German Technical and Scientific Association for Gas and Water (DVGW), Technical rule DVGW G 260 (A), Gas. Quality. (2021).
[24] German Technical and Scientific Association for Gas and Water (DVGW), Technical Rule DVGW G 262 (A): Use of Gases from Renewable Sources in the Public Gas Network, 2021.
[25] Ministry of Industry - Danish Safety Authority, Regulation on Gas Quality, BEK No. 230 of 21/03/2018, 2018.
[26] European Commission, Report on the biomethane injection into national gas grid. https://ec.europa.eu/research/participants/documents/downloadPublic?documentIds=080166e5abba7376&appId=PPGMS, 2016. (Accessed 1 April 2025).
[27] Spanish Electricity Grid (REE), Report on renewable energies. https://www.sistemaelectrico-ree.es/sites/default/files/2024-03/Informe_Renovables_2023.pdf, 2023 (Available only in Spanish).
[28] Suri Marcel, Betak Juraj, Rosina Konstantin, Chrkavy Daniel, Suriova Nada, Cebecauer Tomas, Caltik Marek, Erdelyi Branislav, Global photovoltaic power potential by country. https://documents.worldbank.org/en/publication/documents-reports/documentdetail/466331592817725242/global-photovoltaic-power-potential-by-country, 2022.
[29] Spanish Electricity Grid (REE), Demand evolution, System. Reports. (2023). https://www.sistemaelectrico-ree.es/informe-del-sistema-electrico/demanda/evolucion-demanda.
[30] Energydata.info, Global wind atlas. https://globalwindatlas.info/en/, 2025.
[31] Spanish Gas Association (SEDIGAS), SEDIGAS presents the study on biomethane production capacity in Spain. https://www.sedigas.es/new/comunicado-articulo/sedigas-presenta-el-estudio-de-la-capacidad-de-produccion-de-biometano-en-espana-2023, 2023 (Available only in Spanish).
[32] Naturgy Foundation, Biogas and biomethane as key drivers in the decarbonization of the Spanish economy. https://www.fundacionnaturgy.org/publicacion/el-biogas-y-el-biometano-como-palanca-clave-en-la-descarbonizacion-de-la-economia-espanola/, 2023 (Available only in Spanish).
[33] Boletín Oficial del Estado (BOE), BOE-A-2012-1310 Real Decreto-ley 1/2012, de 27 de enero, por el que se procede a la suspensión de los procedimientos de preasignación de retribución y a la supresión de los incentivos económicos para nuevas instalaciones de producción de energía eléctrica a partir de cogeneración, Fuentes. de Energía. Renovables. y Residuos. (2012). https://www.boe.es/buscar/act.php?id=BOE-A-2012-1310 (Available only in Spanish).
[34] Secretaría de Estado de Energía, Hoja de Ruta del Biogás. https://www.miteco.gob.es/content/dam/miteco/es/energia/files-1/es-es/Novedades/Documents/00HR_Biogas_V6.pdf, 2022 (Available only in Spanish).
[35] S. Daniarta, D. Sowa, P. Błasiak, A.R. Imre, P. Kolasiński, Techno-economic survey of enhancing Power-to-Methane efficiency via waste heat recovery from electrolysis and biomethanation, Renew. Sustain. Energy Rev. 194 (2024), https://doi.org/10.1016/j.rser.2024.114301.
[36] M. De Saint Jean, P. Baurens, C. Bouallou, Parametric study of an efficient renewable power-to-substitute-natural-gas process including high-temperature steam electrolysis, Int. J. Hydrogen Energy 39 (2014) 17024–17039, https://doi.org/10.1016/j.ijhydene.2014.08.091.
[37] S. Park, K. Choi, C. Lee, S. Kim, Y. Yoo, D. Chang, Techno-economic analysis of adiabatic four-stage CO_2 methanation process for optimization and evaluation of power-to-gas technology, Int. J. Hydrogen Energy 46 (2021) 21303–21317, https://doi.org/10.1016/j.ijhydene.2021.04.015.
[38] M. Al-Breiki, Y. Bicer, Techno-economic evaluation of a power-to-methane plant: levelized cost of methane, financial performance metrics, and sensitivity analysis, Chem. Eng. J. 471 (2023), https://doi.org/10.1016/j.cej.2023.144725.
[39] R. De Paolis, V. Bernardini, L.G. Campana, M.V. Ermini, M. Verna, G. Raimondi, G. Spazzafumo, Techno-economic and climate finance assessment of a methanation plant with green hydrogen production and CO_2 recycling in Italy, Int. J. Hydrogen Energy (2024), https://doi.org/10.1016/j.ijhydene.2024.07.137.
[40] M.S. Ghafoori, K. Loubar, M. Marin-Gallego, M. Tazerout, Techno-economic and sensitivity analysis of biomethane production via landfill biogas upgrading and power-to-gas technology, Energy 239 (2022), https://doi.org/10.1016/j.energy.2021.122086.
[41] C. Faria, C. Rocha, C. Miguel, A. Rodrigues, L.M. Madeira, Process intensification concepts for CO_2 methanation – A review, Fuel 386 (2025) 134269, https://doi.org/10.1016/j.fuel.2024.134269.
[42] M. Pérez-Fortes, J.C. Schöneberger, A. Boulamanti, E. Tzimas, Methanol synthesis using captured CO_2 as raw material: techno-economic and environmental assessment, Appl. Energy 161 (2016) 718–732, https://doi.org/10.1016/j.apenergy.2015.07.067.
[43] M. Farajollahi, N. Almasi, A. Zahedi, B. Kanani, Techno-economic analysis of a biogas power plant: moving to sustainable energy supply and green environment through waste management, Process Saf. Environ. Prot. 193 (2025) 1197–1219, https://doi.org/10.1016/j.psep.2024.11.129.
[44] Boletín Oficial del Estado (BOE), BOE-A-2013-185 Resolución de 21 de diciembre de 2012, de la Dirección General de Política Energética y Minas, por la que se modifica el protocolo de detalle PD-01 "Medición, Calidad. y Odorización de Gas" de las Normas. de Gestión. Técnica. del. Sistema. Gasista. (2012). https://www.boe.es/diario_boe/txt.php?id=BOE-A-2013-185 (Available only in Spanish).
[45] Boletín Oficial del Estado (BOE), BOE-A-2018-14557 Resolución de 8 de octubre de 2018, de la Dirección General de Política Energética y Minas, por la que se modifican las normas de gestión técnica del sistema NGTS-06, NGTS-07 y los protocolos de detalle PD-01 y PD-02. https://www.boe.es/diario_boe/txt.php?id=BOE-A-2018-14557, 2018 (Available only in Spanish).
[46] Spanish Electricity Grid (REE), Wind generation | system report. https://www.sistemaelectrico-ree.es/informe-de-energias-renovables/viento/generacion-viento, 2023.
[47] Spanish Electricity Grid (REE), Photovoltaic solar generation | system report. https://www.sistemaelectrico-ree.es/informe-de-energias-renovables/sol/generacion/solar-fotovoltaica-solgeneracion, 2023.
[48] J. Couper, W.R. Penney, J. Fair, S. Walas, Chemical Process Equipment. Selection and Design, third ed., Elsevier Inc., 2012.
[49] A.M.Y. Razak, Gas turbine performance modelling, analysis and optimisation, in: Modern Gas Turbine Systems: High Efficiency, Low Emission, Fuel Flexible Power Generation, Elsevier Ltd., 2013, pp. 423–514, https://doi.org/10.1533/9780857096067.3.423.
[50] K. Coker, R. Sotudeh-Gharebagh, Chemical process engineering volume 1: design, analysis, simulation, integration, and problem solving with microsoft excel-UniSim software for chemical engineers computation, in: Physical Property, Fluid Flow, Equipment and Instrument Sizing, John Wiley & Sons, Inc, 2022.
[51] C. Branan, Rules of Thumb for Chemical Engineers, third ed., Gulf Publishing Company, 2002.
[52] L.P.L.M. Rabou, L. Bos, High efficiency production of substitute natural gas from biomass, Appl. Catal., B 111–112 (2012) 456–460, https://doi.org/10.1016/j.apcatb.2011.10.034.
[53] M. Tommasi, S.N. Degerli, G. Ramis, I. Rossetti, Advancements in CO_2 methanation: a comprehensive review of catalysis, reactor design and process optimization, Chem. Eng. Res. Des. 201 (2024) 457–482, https://doi.org/10.1016/j.cherd.2023.11.060.
[54] S. Mokhatab, W.A. Poe, J.Y. Mak, Natural gas treating, in: Handbook of Natural Gas Transmission and Processing, Elsevier, 2019, pp. 231–269, https://doi.org/10.1016/b978-0-12-815817-3.00007-1.
[55] J.-G. Lu, Y.-F. Zheng, D.-L. He, Selective absorption of H2S from gas mixtures into aqueous solutions of blended amines of methyldiethanolamine and 2-tertiarybutylamino-2-ethoxyethanol in a packed column, Sep. Purif. Technol. 52 (2006) 209–217, https://doi.org/10.1016/j.seppur.2006.04.003.
[56] S. Shiva Kumar, H. Lim, An overview of water electrolysis technologies for green hydrogen production, Energy Rep. 8 (2022) 13793–13813, https://doi.org/10.1016/j.egyr.2022.10.127.
[57] A.S. Emam, M.O. Hamdan, B.A. Abu-Nabah, E. Elnajjar, A review on recent trends, challenges, and innovations in alkaline water electrolysis, Int. J. Hydrogen Energy 64 (2024) 599–625, https://doi.org/10.1016/j.ijhydene.2024.03.238.
[58] S.G. Nnabuife, A.K. Hamzat, J. Whidborne, B. Kuang, K.W. Jenkins, Integration of renewable energy sources in tandem with electrolysis: a technology review for green hydrogen production, Int. J. Hydrogen Energy (2024), https://doi.org/10.1016/j.ijhydene.2024.06.342.
[59] A.H. Reksten, M.S. Thomassen, S. Møller-Holst, K. Sundseth, Projecting the future cost of PEM and alkaline water electrolysers; a CAPEX model including electrolyser plant size and technology development, Int. J. Hydrogen Energy 47 (2022) 38106–38113, https://doi.org/10.1016/j.ijhydene.2022.08.306.
[60] M. Sterner, M. Specht, Power-to-Gas and power-to-X—the history and results of developing a new storage concept, Energies (Basel) 14 (2021) 6594, https://doi.org/10.3390/en14206594.
[61] M. Felgenhauer, T. Hamacher, State-of-the-art of commercial electrolyzers and on-site hydrogen generation for logistic vehicles in South Carolina, Int. J. Hydrogen Energy 40 (2015) 2084–2090, https://doi.org/10.1016/j.ijhydene.2014.12.043.
[62] W. Li, H. Tian, L. Ma, Y. Wang, X. Liu, X. Gao, Low-temperature water electrolysis: fundamentals, progress, and new strategies, Mater. Adv. 3 (2022) 5598–5644, https://doi.org/10.1039/d2ma00185c.
[63] G. Chisholm, L. Cronin, Hydrogen from water electrolysis, in: Storing Energy: with Special Reference to Renewable Energy Sources, Elsevier Inc., 2016, pp. 315–343, https://doi.org/10.1016/B978-0-12-803440-8.00016-6.
[64] G. Iaquaniello, S. Setini, A. Salladini, M. De Falco, CO_2 valorization through direct methanation of flue gas and renewable hydrogen: a technical and economic assessment, Int. J. Hydrogen Energy 43 (2018) 17069–17081, https://doi.org/10.1016/j.ijhydene.2018.07.099.
[65] T. Schildhauer, S. Biollaz, The power to gas process: storage of renewable energy in the natural gas grid via fixed bed methanation of CO_2/H_2, in: Synthetic Natural Gas from Coal, Dry Biomass, and Power-To-Gas Applications, John Wiley & Sons, Inc., 2016, pp. 191–219.
[66] S. Farsi, W. Olbrich, P. Pfeifer, R. Dittmeyer, A consecutive methanation scheme for conversion of CO_2 – a study on Ni_3Fe catalyst in a short-contact time micro packed bed reactor, Chem. Eng. J. 388 (2020) 124233, https://doi.org/10.1016/j.cej.2020.124233.
[67] J. Carroll, Dehydration of natural gas, in: Natural Gas Hydrates, Elsevier, 2020, pp. 209–231, https://doi.org/10.1016/B978-0-12-821771-9.00006-9.
[68] F. Manning, R. Thompson, Gas dehydration using glycol, in: Oilfield Processing of Petroleum: Natural Gas, PennWell Publishing Company, 1991, pp. 139–169.
[69] A.M. Braek, R.A. Almehaideb, N. Darwish, R. Hughes, Optimization of process parameters for glycol unit to mitigate the emission of BTEX/VOCs, Process Saf. Environ. Prot. 79 (2001) 218–232, https://doi.org/10.1205/095758201750362262.

[70] M.I. Stewart, Dehydration, in: Surface Production Operations, Elsevier, 2014, pp. 279–373, https://doi.org/10.1016/B978-0-12-382207-9.00007-X.
[71] W.D. Seider, D.R. Lewin, J.D. Seader, S. Widagdo, R. Gani, K.M. Ng, Product and Process Design Principles. Synthesis, Analysis and Evaluation, fourth ed., John Wiley & Sons Inc., 2016.
[72] R.M. Busche, Venture Analysis: A Framework for Venture Planning - Course Notes, Bio-En-Gene-Er Associates, 1995.
[73] K.M. Guthrie, Process Plant Estimating Evaluation and Control, Craftsman Book Company, 1974.
[74] I. Explore, Independent commodity intelligence services | ICIS. https://www.icis.com/explore/, 2025.
[75] BusinessAnalytiq, Potassium hydroxide price index, in: https://businessanalytiq.com/procurementanalytics/index/potassium-hydroxide-price-index/, 2023.
[76] G. Towler, R. Sinnott, Costing and project evaluation, in: Chemical Engineering Design: Principles, Practice and Economics of Plant and Process Design, Butterworth-Heinemann, 2007, pp. 297–392.
[77] Spanish Electricity Grid (REE), Final avarage price | system files. https://www.sistemaelectrico-ree.es/informe-del-sistema-electrico/mercados/precio-medio-final, 2023.
[78] National Statistics Institute (INE), Decile of salaries from main employment, Labour. Force. Survey (LFS). (2023). https://ine.es/dyngs/Prensa/es/dsEPA2023.htm.
[79] Iberian Gas Market (MIBGAS), Annual report of the organized gas market. https://www.mibgas.es/sites/default/files/MIBGAS_informe_anual_2023.pdf, 2023 (Available only in Spanish).
[80] Iberian Gas Market (MIBGAS), MIGBAS, IBHYX Index. (2025). https://greenenergy.mibgas.es/.
[81] Iberian gas market (MIBGAS), file access | MIBGAS. https://www.mibgas.es/es/file-access, 2023.
[82] S. Michailos, M. Walker, A. Moody, D. Poggio, M. Pourkashanian, Biomethane production using an integrated anaerobic digestion, gasification and CO_2 biomethanation process in a real wastewater treatment plant: a techno-economic assessment, Energy Convers Manag 209 (2020) 112663, https://doi.org/10.1016/j.enconman.2020.112663.
[83] L. Menin, K. Asimakopoulos, S. Sukumara, N.B.K. Rasmussen, F. Patuzzi, M. Baratieri, H.N. Gavala, I.V. Skiadas, Competitiveness of syngas biomethanation integrated with carbon capture and storage, power-to-gas and biomethane liquefaction services: techno-economic modeling of process scenarios and evaluation of subsidization requirements, Biomass Bioenergy 161 (2022) 106475, https://doi.org/10.1016/j.biombioe.2022.106475.
[84] J. Casey, Solar stabilisation: in conversation with LevelTen on its latest European PPA report. https://www.pv-tech.org/solar-stabilisation-in-conversation-levelten-latest-european-ppa-report/, 2024.
[85] L. Bühler, D. Möst, Projecting technological advancement of electrolyzers and the impact on the competitiveness of hydrogen, Int. J. Hydrogen Energy 98 (2025) 1174–1184, https://doi.org/10.1016/j.ijhydene.2024.12.078.
[86] Pexapark, European PPA market outlook 2024. https://pexapark.com/european-ppa-market/, 2024.
[87] Ministerio para la Transición Ecológica y el Reto Demográfico (MITECO), Plan Nacional Integrado de Energía y Clima (PNIEC 2023-2030). https://www.miteco.gob.es/content/dam/miteco/es/energia/files-1/pniec-2023-2030/PNIEC_2024_240924.pdf, 2024 (Available only in Spanish).
[88] S. Krishnan, V. Koning, M. Theodorus de Groot, A. de Groot, P.G. Mendoza, M. Junginger, G.J. Kramer, Present and future cost of alkaline and PEM electrolyser stacks, Int. J. Hydrogen Energy 48 (2023) 32313–32330, https://doi.org/10.1016/J.IJHYDENE.2023.05.031.
[89] National Commission on Markets and Competition (CNMC), Supervision report on the iberian peninsula's wholesale spot electricity market. https://www.cnmc.es/sites/default/files/5177925.pdf, 2024 (Available only in Spanish).